metals

MDPI

Article

Effects of Mg Addition and Pre-Aging on the Age-Hardening Behavior in Al-Mg-Si

JaeHwang Kim *, Jiwoo Im, Minyoung Song and Insu Kim

Carbon and Light Materials Application R&D Group, Korea Institute of Industrial Technology, 222, Palbok-ro, Deokjin-gu, Jeonju-City 54853, Korea; tjd91@kitech.re.kr (J.I.); minyoung098@kitech.re.kr (M.S.); ujm896@kitech.re.kr (I.K.)

* Correspondence: raykim@kitech.re.kr; Tel.: +82-63-210-3715

Received: 20 November 2018; Accepted: 7 December 2018; Published: 10 December 2018

Abstract: Two types of nanoclusters, Cluster (1) and Cluster (2), formed at around room temperature and 100 °C, respectively, affect the age-hardening behavior in Al-Mg-Si alloys. Formation of Cluster (1) during natural aging (NA) is more accelerated in the high-Mg (9M10S) alloy than in the low-Mg (3M10S) alloy. Hardness at the early stage of two-step aging at 170 °C is not increased for the natural aging samples. On the other hand, hardness is directly increased for the pre-aged (PA) specimens. Furthermore, the formation of Cluster (1) during natural aging is suppressed by the formation of Cluster (2) during pre-aging at 100 °C. To understand the effects of heat treatment histories and Mg contents on the microstructure, transmission electron microscopy (TEM) was utilized. All the images were obtained at (001) plane, and peak aged samples with different heat treatments were used. Lower number density of precipitates is confirmed for the natural aging samples compared with the single-aged and pre-aged specimens. A higher number density of precipitates is confirmed for 9M10S in comparison to 3M10S. Hardness results correspond well to the TEM images.

Keywords: Al-Mg-Si alloys; age-hardening; precipitates; pre-aging; Mg addition

1. Introduction

Al-Mg-Si alloys have been used for the body panels of automobiles due to their good age-hardening response, formability and corrosion resistance. The precipitation sequence in Al-Mg-Si alloys is

$$\text{SSS} \rightarrow \text{GP Zone} \rightarrow \beta'' \rightarrow \beta', \text{U1, U2, B}' \rightarrow \beta \quad (1)$$

where SSS and β represent the super-saturated solid solution and an equilibrium phase, respectively [1,2]. SSS can be formed through solid solution treatment. The energetically stable β phase, compared with metastable phases such as GP Zone, β″ and β′, can be obtained with a prolonged aging treatment. Recently, atomic-scale analysis has become possible with the development of equipment. Information on the chemical composition and the size distribution of nanoclusters has been reported using a three-dimensional atom probe (3DAP) in Al-Mg-Si alloys [3–6]. Generally, Al-Mg-Si sheets are delivered from aluminum companies to automobile companies and are stored at room temperature. Finally, the Al-Mg-Si sheets are pressed into the design of the automobile, and the paint bake process is carried out. The paint bake process is usually conducted at around 170 °C for 1200 s. Bake hardening (BH) response is quite important in Al-Mg-Si alloys to enhance the strength of aluminum alloys in consideration of the production process.

The two-step aging behavior of Al-Mg-Si alloys has been extensively reported, since the commercial processes, transformation and storage of aluminum sheets and paint bake process are comprised of two-step heat treatments, i.e., natural aging (NA) and artificial aging (AA). Pashely et al. described the negative effects of two-step aging in Al-Mg-Si alloys [7]. The term 'negative effects of two-step aging'

refers to the decrease in mechanical properties during two-step aging when natural aging is performed before isothermal aging, in comparison to single-step aging. This phenomenon is closely related to the role of nanoclusters formed during natural aging in two-step aging. Serizawa et al. clarified that there are two types of nanoclusters [8]. Cluster (1) and Cluster (2) are formed at around room temperature and 100 °C, respectively, based on three-dimensional atom probe (3DAP) analyses. Kim et al. confirmed that nanoclusters are strongly affected by the chemical composition [9,10]. However, the effects of chemical composition with the heat treatments on the age-hardening behavior have been poorly understood. Al-Mg-Si alloys with high and low Mg content were used, and the pre-aging (PA) in this study was designed to investigate the influence of Mg content on the age-hardening behavior and the role of nanoclusters in the two-step and multi-step aging behaviors of Al-Mg-Si alloys.

2. Materials and Methods

Two kinds of Al-Mg-Si alloys, 3M10S (low Mg) and 9M10S (high Mg) alloys, supplied by UACJ Corp, were used in this study. The details of the chemical compositions are described in Table 1. All specimens were solution-treated using a salt bath at 560 °C for 1800 s and quenched in ice-water at 0 °C for 60 s. Natural aging is performed at room temperature around 25 °C. Pre-aging is conducted at 100 °C for 3600 s using an oil bath in order to understand the effects of the pre-aging on the multi-step aging behavior. Isothermal aging was carried out at 170 °C using an oil bath. Micro Vickers hardness measurements were employed with a load of 200 g for 10 s using Mitsutoyo HV-113 (Mitutoyo, Kanagawa, Japan) in order to measure the mechanical property with the heat treatments. An average of five out of seven hardness results were used. The size of the specimen was 10 mm × 10 mm, with a thickness of 10 mm. All the hardness measurements were performed within 300 s after heat treatment to minimize clustering during the exposure time at room temperature. Thermal analyses were performed using NETZSCH DSC 204 F1 (NETZSCH, Selb, Germany) phoenix equipment with a heating rate of 0.33 °C/s under a nitrogen atmosphere. To analyze the clustering behavior, the DSC was started at −50 °C using liquid nitrogen with a diameter of 3 mm. The specimens for the observation by transmission electron microscopy (TEM) were electro-polished using Struers-Tenopol-5 (Struers, Ballerup, Denmark) with solution (33 vol % HNO_3 + 67 vol % CH_3OH) at −30 °C in order to observe the nano-precipitates using JEM-2010 (JEOL, Tokyo, Japan) with 200 kV accelerating voltage.

Table 1. Chemical compositions used in this study.

Materials	Mg	Si	Al	Mg/Si
9M4S	0.9	0.4	Bal.	2.5
6M6S	0.6	0.6	Bal.	1
3M10S	0.3	1.0	Bal.	0.3

3. Results

3.1. Thermal Analyses

Figure 1 shows the DSC results of the as-quenched 9M10S and 3M10S specimens. One endothermic and four exothermic peaks are identified ranging from 0 to 500 °C. The exothermal peaks are considered to be the formation of nanoclusters, with β″, β′ and β phases being indicated by peaks I, III, IV and V, respectively. Peak II is attributed to the dissolution of nanoclusters formed during DSC running. These results are in good agreement with previously obtained results [11,12]. Two overlapping peaks appeared, ranging from 0 to 150 °C, as indicated by arrows for both the 9M10S and 3M10S samples, as shown in Figure 1b. The overlapping peaks are well separated by the Gaussian function method, as shown in Figure 1c,d. The multiple peaks were fitted by the parameters such as the number and center of peaks based on the following equation:

$$y = y_0 + \frac{A}{w\sqrt{\pi - 2}} e^{-2\frac{(x-x_c)}{w^2}}$$

where y_0, x_c, w and A stand for bottom, center, width and area of the peak. Serizawa et al. confirmed two types of nanoclusters, i.e., Cluster (1) and Cluster (2), based on thermal and 3DAP analyses [8]. The separated peaks corresponded to Cluster (1) and Cluster (2), as shown in Figure 1c,d, respectively.

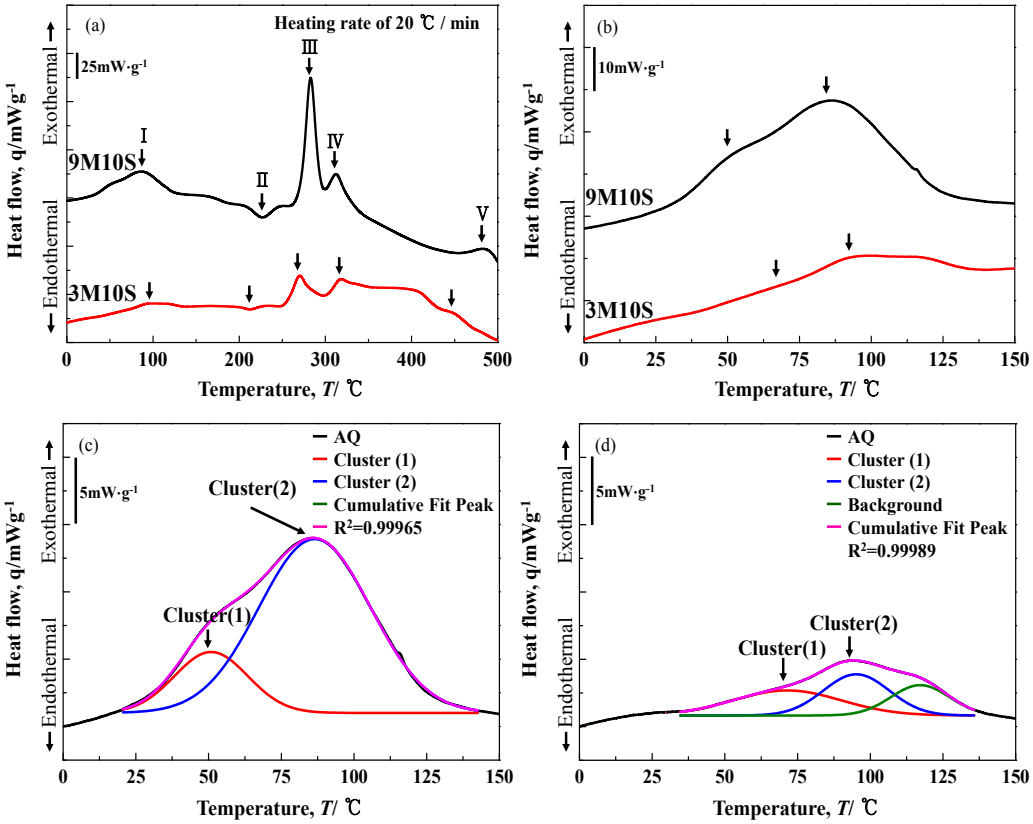

Figure 1. Differential scanning calorimetry (DSC) curves over the full range of the as-quenched specimens during a heating rate of 0.33 °C/s in the 9M10S (**a**) and 3M10S (**b**). The overlapped peaks were separated through the Gaussian function method for 9M10S (**c**) and 3M10S (**d**).

3.2. Mechanical Properties

3.2.1. Clustering and Age-Hardening Behavior with Mg Addition

Nanoclusters are formed during low-temperature aging, and they affect the subsequent age-hardening behavior. Nanoclusters are comprised of solute atoms, such as Mg and Si atoms, and vacancies. To understand the formation behavior of Cluster (1) with Mg addition, natural aging is performed with the different Mg contents. Figure 2 shows the hardness results during natural aging in the 3M10S and 9M10S. The hardness is basically increased due to the formation of Cluster (1) during natural aging. Higher hardness is confirmed in the 9M10S than in the 3M10S. It is noted that the formation of Cluster (1) is more accelerated by Mg addition based on the hardness results during natural aging. Meanwhile, Cluster (2) is formed at around 100 °C [8]. Pre-aging is performed before natural aging to understand the effect of clustering on the following aging behavior. Figure 3 shows the hardness results during aging at 170 °C after PA-NA or NA. Hardness is increased during pre-aging due to the formation of Cluster (2). Higher hardness during pre-aging is confirmed in the 9M10S than in the 3M10S. It is noted that the formation of Cluster (2) is enhanced by Mg addition. Also, the higher hardness during single aging indicated by the black line is analyzed in the 9M10S compared with 3M10S, as shown in Figure 3. This means that the formation of precipitates is accelerated by Mg addition. As displayed by the black line, hardness is directly increased during aging at 170 °C, but there is a retardation of hardness increase at the early stage of aging at 170 °C for the natural aging samples, regardless of chemical composition. On the other hand, hardness is directly increased for the

pre-aging specimens. The β″ phase is generally formed during aging at 170 °C [11]. It is noted that Cluster (1) formed during natural aging does not directly transform into the β″ phase, but Cluster (2) transforms into the β″ phase during aging at 170 °C. In the case of 3M10S, a similar peak hardness is identified between the PA-NA, NA-AA and single-aged specimens. On the other hand, the highest and lowest peak hardnesses are observed in the 9M10S for the single-aged and natural aging specimens, respectively. To clearly understand the effects of cluster formation on the following aging treatment, the hardness difference is calculated. The hardness difference is obtained from the difference between the hardness during isothermal aging at 170 °C and before isothermal (BI) aging. Namely, the BI condition corresponds to the hardness value after NA or PA-NA. Figure 4 shows the hardness difference during aging at 170 °C with the different heat treatment histories. BI on the horizontal axis in Figure 4 stands for before isothermal aging at 170 °C. The different age-hardening behavior under different pre-aging conditions is clearly revealed. The retardation period of the hardness increase is clearly identified only in the natural aging specimens. Interestingly, a larger difference is observed in the 3M10S than in the 9M10S under the natural aging condition, but a similar hardness difference is observed between 3M10S and 9M10S in the case of pre-aging samples. It is noted that the competitively formed nanoclusters during natural aging or pre-aging strongly affect the age-hardening behaviors during two-step or multi-step aging. The details of those phenomena are discussed in the next section.

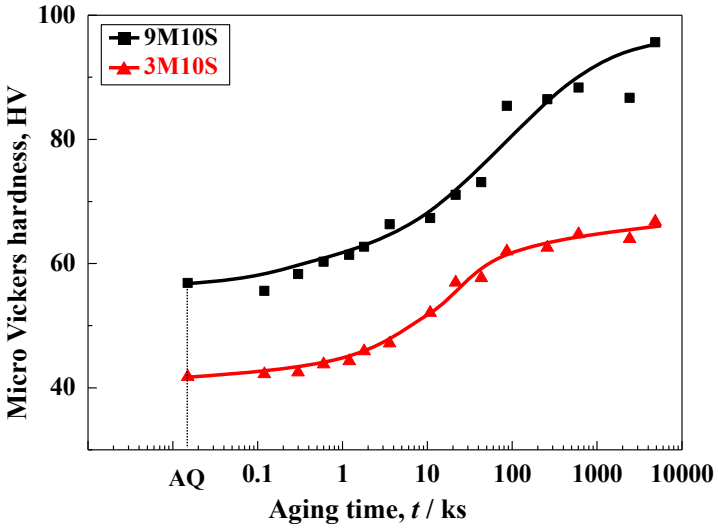

Figure 2. Hardness changes during natural aging in the 3M10S and 9M10S. AQ represents as-quenched.

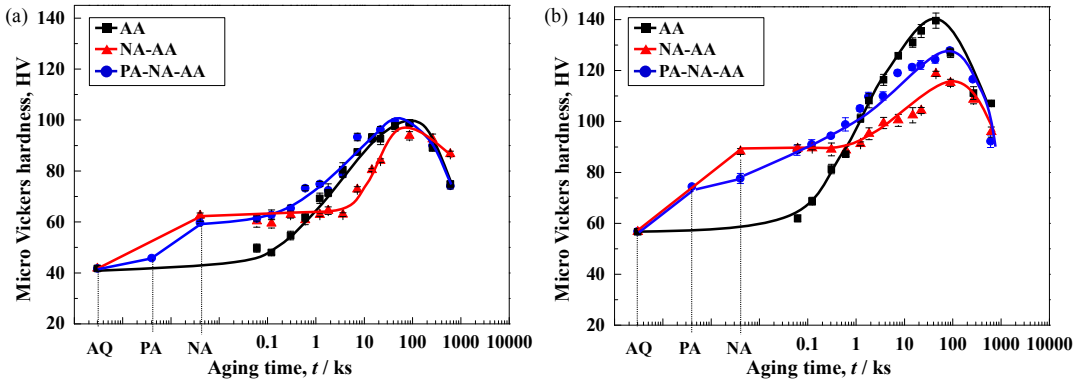

Figure 3. Hardness during aging at 170 °C with the different heat treatments in (**a**) 3M10S and (**b**) 9M10S. AQ, PA, NA and AA stand for as-quenched, pre-aging at 100 °C for 3600 s, natural aging at room temperature for 7 days, and artificial aging at 170 °C, respectively.

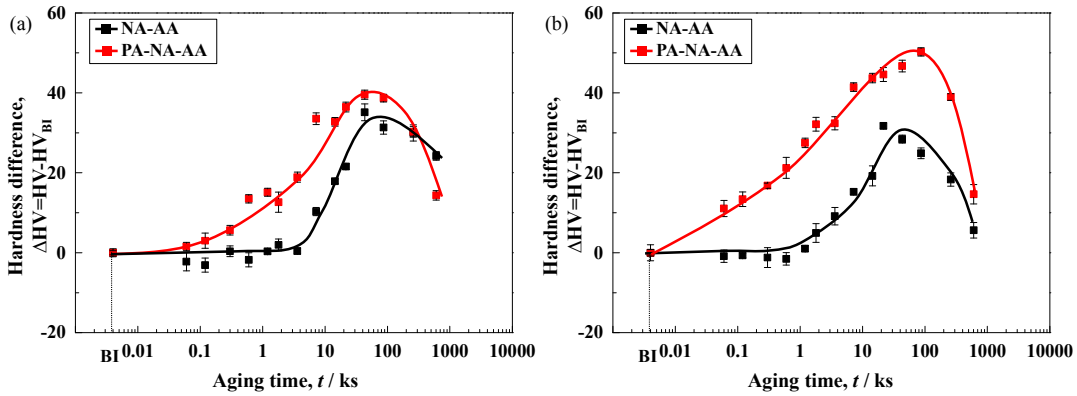

Figure 4. Hardness difference during two-step and multi-step aging at 170 °C in (**a**) 3M10S and (**b**) 9M10S. Hardness difference is defined as the difference value of the obtained hardness during the two-step or multi-step aging at 170 °C from the hardness value at the state of PA-NA or NA. BI, NA, PA and AA stand for before isothermal aging at 170 °C, natural aging for 7 days, presaging at 100 °C, and artificial aging at 170 °C, respectively.

3.2.2. Clustering and Bake-Hardening Response

The paint-bake process is generally conducted at around 170 °C for 1200 s. The enhancement of the mechanical properties is quite important in the early stage of final aging due to the limited production process. Figure 5 shows the hardness changes in consideration of the paint-bake process. There is a hardness increase during natural aging due to the formation of Cluster (1) in the case of the natural aging specimen, as shown in blue. The hardness increase for the bake hardening condition is displayed in red. There is little increase in hardness in 3M10S during bake hardening for the natural aging specimen. Additionally, a slight increase in hardness is confirmed in the 9M10S. Smaller bake hardening responses are confirmed in the natural aging samples than in the single aged ones for both 3M10S and 9M10S. On the other hand, a hardness increase due to the formation of Cluster (2) during pre-aging is observed, and is shown in green. Importantly, the hardness increase due to the formation of Cluster (1) during natural aging after pre-aging is clearly suppressed. Higher and lower hardnesses are observed in the pre-aging and natural aging samples, respectively, than in the single-aged samples. It is noted that the positive and negative aging behaviors are found to be due to the competitively formed nanoclusters. The bake hardening response is markedly affected by the clustering during low temperature aging.

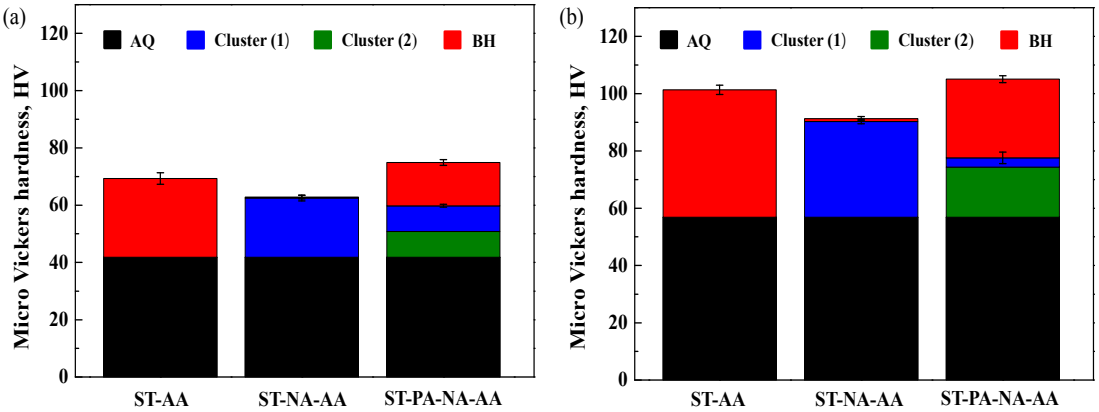

Figure 5. Hardness changes with each step of heat treatment in the (**a**) 3M10S and (**b**) 9M10S. AQ, ST, PA, NA, AA and BH stand for as-quenched, solid solution heat-treated, pre-aged at 100 °C for 3600 s, naturally aged for 7 days, artificially aged at 170 °C for 1200 s, and bake hardening response, respectively.

3.3. Microstructure

The Al-Mg-Si alloys are mainly strengthened by precipitate formation. Figure 6 shows TEM micrographs with different chemical composition and heat treatment histories. All images were finally and obtained at (001) plane in Al matrix after being aged at 170 °C for 43,200 s (12 h), as shown in selected area diffraction pattern (SADP). The red circle area of Figure 6b was enlarged in order to understand the structure of the precipitate. The precipitate is identified as the β″ phase based on the structure analysis, as shown in the upper right side of Figure 6b. A similar method for the structural analysis of precipitates based on TEM images has been introduced previously [2,13]. A higher number density of the β″ phase is observed in the 9M10S than in the 3M10S for the directly aged samples. It is noted that β″ phase formation is enhanced by Mg addition. In the case of naturally aged samples, a lower number density of the β″ phase is identified for the naturally aged samples than for the single-aged one regardless of chemical composition. This means that formation of Cluster (1) during natural aging interferes with the formation of β″ phase during two-step aging. A lower number density is observed in the 9M10S than in the 3M10S for the naturally aged samples. Detailed reasons for this will be discussed in the next section. Meanwhile, higher number densities of precipitates are observed for the pre-aged samples in the both 9M10S and 3M10S than in the naturally aged samples. This means that the formation of β″ phase is accelerated by the formation of Cluster (2).

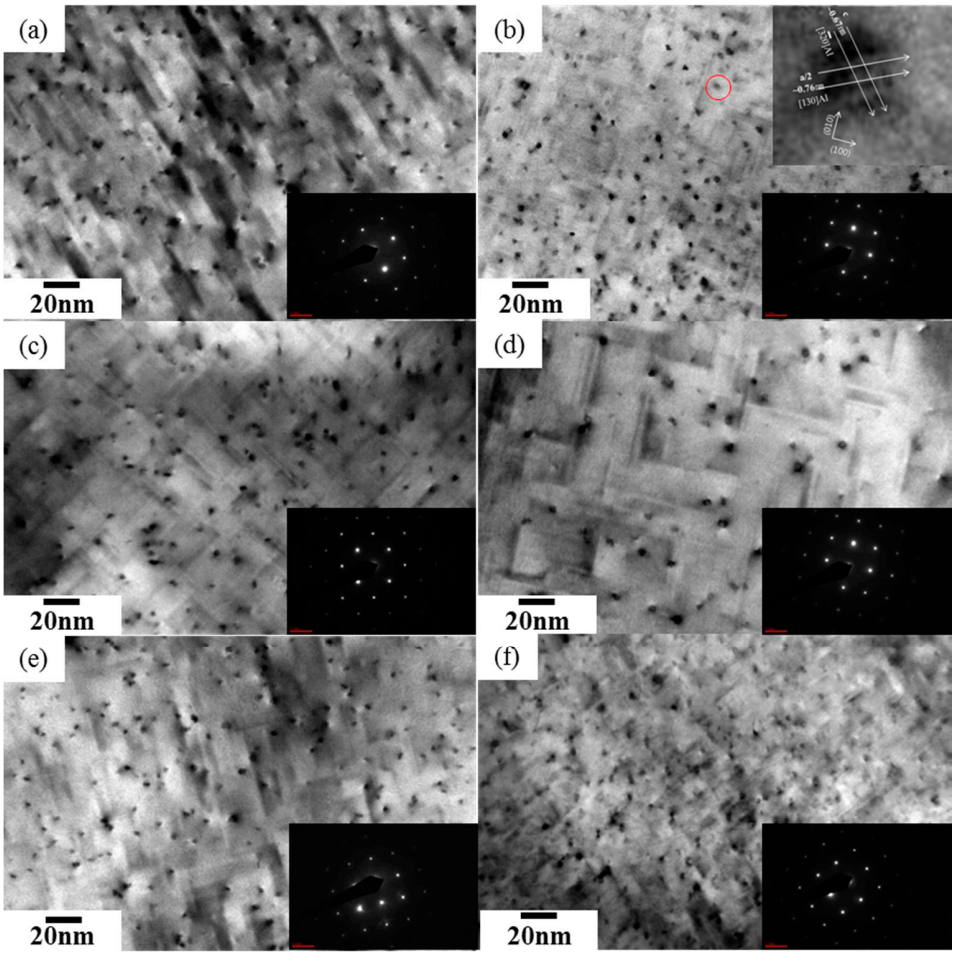

Figure 6. TEM micrographs with different heat treatments in 3M10S and 9M10S. (**a**) AA, (**c**) NA-AA, and (**e**) PA-NA-AA in 3M10S; and (**b**) AA, (**d**) NA-AA, and (**f**) PA-NA-AA in 9M10S. NA, PA, and AA stand natural aging at room temperature for 7 days, pre-aging at 100 °C for 3600 s, and artificial aging at 170 °C for 43,200 s (12 h), respectively. The precipitate is identified as the β″ phase based on structure analysis as shown in upper right of (**b**).

4. Discussion

4.1. Clustering Behavior with Mg Addition

The negative effects of two-step aging, such as the decrease in mechanical properties, are generally accepted in Al-Mg-Si alloys [14,15]. This phenomenon is caused by the formation of nanoclusters during natural aging. The clustering behavior is strongly affected by the chemical composition [9,10]. Also, the chemical composition and the size of nanoclusters are affected by the heat treatment histories [16,17]. Firstly, higher hardness is confirmed during natural aging in the high-Mg-content alloy (9M10S) than in the low-Mg-content alloy (3M10S), as shown in Figure 2. Also, higher hardness after pre-aging is confirmed in the 9M10S than in the 3M10S, as shown in Figure 3. This means that the formation of Cluster (1) and Cluster (2) is enhanced by Mg addition. After pre-aging, both alloys were naturally aged for 7 days. The hardness during natural aging after pre-aging is increased by 3.2 and 9 HV for the 9M10S and 3M10S, respectively. The hardness increase is lower in the 9M10S than in the 3M10S. It is interesting that the formation of Cluster (1) is strongly suppressed due the formation of Cluster (2) during pre-aging. It is noted that nanoclusters are competitively formed based on the results of the hardness increase during natural aging after pre-aging. At this moment, it is not yet clear whether the second hardness increase during natural aging after pre-aging is caused by the formation of Cluster (1) in the Al matrix, or the growth of Cluster (2). Further research using three-dimensional atom probes is required to clarify the mechanism of hardness increase during natural aging after pre-aging.

4.2. Clustering and Final Aging Behavior

It is very useful to obtain a high number of nuclei in the precipitate for the enhancement of the mechanical properties in the age-hardenable Al alloys. In other words, high-strength Al alloy can be obtained if all the nanoclusters formed during low-temperature pre-aging play a role in the nuclei of the precipitate. However, not all the clusters transfer to the strengthening phase in Al-Mg-Si alloys. Meanwhile, the initial stage of two-step aging is strongly affected by the cluster formation, as shown in Figure 3. This means that control of the cluster formation is quite important in Al-Mg-Si alloys when considering the bake hardening condition. The second hardness increase during natural aging after pre-aging is suppressed, resulting in a higher bake hardening response being observed in the 9M10S than in the 3M10S, as shown in Figure 5. The negative and positive effects on bake hardening response were confirmed to be due to the formation of different types of nanoclusters.

Higher hardness is identified in the 9M10S than in the 3M10 for NA-AA and PA-NA-AA, as shown in Figure 3. The hardness difference is calculated in this study as shown in Figure 4. Interestingly, a lower increase is confirmed in the 9M10S than in the 3M10S for the NA-AA. It is probable that there are fewer opportunities to form the β″ phase since more solute atoms, such as Mg and Si atoms, and vacancies were consumed during natural aging. That is why the lower number density of the β″ phase is observed in the 9M10S than in the 3M10 based on TEM images, as shown in Figure 6. With his, control of nanoclusters is quite important in Al-Mg-Si alloys, since the nanoclusters formed at low temperatures strongly affect the bake-hardening response and final age-hardening behavior of Al-Mg-Si alloys.

5. Conclusions

The influence of Mg addition and pre-aging on the age-hardening behavior in Al-Mg-Si is discussed based on the experimentally obtained hardness and TEM results.

(1) Formation of nanoclusters such as Cluster (1) and Cluster (2) and the β″ phase is accelerated by Mg addition, based on hardness tests and TEM observation.

(2) Formation of Cluster (1) is suppressed by the formation of Cluster (2) through pre-aging at 100 °C. The negative effect of the two-step aging is suppressed and the bake-hardening response is clearly enhanced through the pre-aging treatment. Higher number density of the β″ phase is observed in the pre-aging specimen than that of the natural aging one, based on TEM images.

(3) The hardness difference during two-step aging for the natural aging samples is lower in the 9M10S (high-Mg-content alloy) than in the 3M10S (low-Mg-content alloy), since more solute atoms and vacancies are consumed during natural aging for the formation of Cluster (1) by Mg addition.

Author Contributions: J.K. designed the experiments; J.I., M.S., and I.K. performed the experiments; J.K. analyzed the data; J.K. wrote the paper; J.K. reviewed and edited.

Funding: This work was supported by the research of Development of hot/warm forming-heat treatment integrated process for high strength aluminum alloy (PEO18272) from Korea Institute of Industrial Technology. The present authors are grateful to UACJ Corp. for the material supply. TEM samples were analyzed by TEM (JEM-2010) installed in the Center for University-Wide Research Facilities (CURF) at Chonbuk National University.

Conflicts of Interest: The authors declare no conflict of interest.

References

1. Matsuda, K.; Sakaguchi, Y.; Miyata, Y.; Uetani, Y.; Sato, T.; Kamio, A.; Ikeno, S. Precipitation sequence of various kinds of metastable phases in Al-1.0mass% Mg_2Si-0.4mass% Si alloy. *J. Mater. Sci.* **2000**, *35*, 179–189. [CrossRef]
2. Marioara, C.D.; Andersen, S.J.; Zandbergen, H.W.; Holmestad, R. The Influence of Alloy Composition on Precipitates of the Al-Mg-Si System. *Metall. Mater. Trans. A* **2005**, *36*, 691–702. [CrossRef]
3. Rometsch, P.A.; Cao, L.F.; Xiong, X.Y.; Muddle, B.C. Atom probe analysis of early-stage strengthening behaviour in an Al–Mg–Si–Cu alloy. *Ultramicroscopy* **2011**, *111*, 690–694. [CrossRef] [PubMed]
4. Pogatscher, S.; Antrekowitsch, H.; Leitner, H.; Sologubenko, A.S.; Uggowitzer, P.J. Influence of the thermal route on the peak-aged microstructures in an Al–Mg–Si aluminum alloy. *Scr. Mater.* **2013**, *68*, 158–161. [CrossRef]
5. Cao, L.; Rometsch, P.A.; Couper, M.J. Effect of pre-ageing and natural ageing on the paint bake response of alloy AA6181A. *Mater. Sci. Eng. A* **2013**, *571*, 77–82. [CrossRef]
6. Geuser, F.D.; Lefebvrea, W.; Blavettea, D. 3D atom probe study of solute atoms clustering during natural ageing and pre-ageing of an Al-Mg-Si alloy. *Philos. Mag. Lett.* **2006**, *86*, 227–234. [CrossRef]
7. Pashley, D.W.; Rhodes, J.W.; Sendorek, A. Delayed ageing in Aluminum-Magnesium-Silicon Alloys: Effect of structure and Mechanical Properties. *J. Inst. Met.* **1996**, *94*, 41–49.
8. Serizawa, A.; Hirosawa, S.; Sato, T. Three-Dimensional Atom Probe Characterization of Nanoclusters Responsible for Multistep Aging Behavior of an Al-Mg-Si Alloy. *Metall. Mater. Trans. A* **2008**, *39A*, 243–251. [CrossRef]
9. Kim, S.; Kim, J.; Tezuka, H.; Kobayashi, E.; Sato, T. Formation Behavior of Nanoclusters in Al-Mg-Si alloys with Different Mg and Si concentration. *Mater. Trans.* **2013**, *54*, 297–303. [CrossRef]
10. Kim, S.; Kim, J.; Kobayashi, E.; Sato, T. Influence of Mg/Si Ratio on Nanocluster Formation in Al-Mg-Si Alloys with Constant Mg + Si Concentration. *Mater. Trans.* **2014**, *55*, 1647–1655. [CrossRef]
11. Miao, W.F.; Laughlin, D.E. Effects of Cu content and preaging on precipitation characteristics in aluminum alloy 6022. *Metall. Mater. Trans.* **2000**, *31A*, 361–371. [CrossRef]
12. Gaber, A.; Gaffar, M.A.; Mostafa, M.S.; Zeid, E.F.A. Precipitation kinetics of Al–1.12 Mg_2Si–0.35 Si and Al–1.07 Mg_2Si–0.33 Cu alloy. *J. Alloy. Comp.* **2007**, *429*, 167–175. [CrossRef]
13. Kim, J.; Marioara, C.D.; Holmestad, R.; Kobayashi, E.; Sato, T. Effects of Cu and Ag addition on the age-hardening behavior during multi-step aging in Al-Mg-Si alloys. *Mater. Sci. Eng. A* **2013**, *560*, 154–162. [CrossRef]
14. Pashley, D.W.; Jacobs, M.H.; Vietz, J.T. The basic processes affecting two-step ageing in an Al-Mg-Si alloy. *Philos. Mag.* **1967**, *51*, 51–76. [CrossRef]
15. Marioara, C.D.; Andersen, S.J.; Jansen, J.; Zandbergen, H.W. The influence of temperature and storage time at RT on nucleation of the β″ phase in a 6082 Al–Mg–Si alloy. *Acta Mater.* **2003**, *51*, 789–796. [CrossRef]

16. Aruga, Y.; Kozuka, M.; Takaki, Y.; Sato, T. Effects of natural aging after pre-aging on clustering and bake-hardening behavior in an Al–Mg–Si alloy. *Scr. Mater.* **2016**, *116*, 82–86. [CrossRef]
17. Aruga, Y.; Kozuka, M.; Sato, T. Formulation of initial artificial age-hardening response in an Al-Mg-Si alloy based on the cluster classification using a high-detection efficiency atom probe. *J. Alloy. Compd.* **2018**, *739*, 1115–1123. [CrossRef]